THE JOURNAL OF PHYSICAL CHEMISTRY Letters

Letter

pubs.acs.org/JPCL

Criegee Chemistry on Aqueous Organic Surfaces

Shinichi Enami*,† and A. J. Colussi*,‡

†National Institute for Environmental Studies, 16-2 Onogawa, Tsukuba, Ibaraki 305-8506, Japan

‡Linde Center for Global Environmental Science, California Institute of Technology, Pasadena, California 91125, United States

Supporting Information

ABSTRACT: In the troposphere, the fate of gas-phase Criegee intermediates (CIs) is deemed to be determined by their reactions with water molecules. Here it is shown that CIs produced in situ on the surface of water/acetonitrile (W/AN) solutions react competitively with millimolar carboxylic acids. Present experiments probe, via online electrospray mass spectrometry, CIs' chemistry on the surface of α-humulene and β-caryophyllene in W/AN microjets exposed to $O_3(g)$ for <10 μs. Mass-specific identification lets us establish the progeny of products and intermediates generated in the early stages of CIs' reactions with H_2O, D_2O, $H_2{}^{18}O$, and n-alkyl-COOH (n = 1−7). It is found that n-alkyl-COOH competes for CIs with interfacial water, their competitiveness being an increasing function of n. Present findings demonstrate that CIs can react with species other than H_2O on the surface of aqueous organic aerosols due to the low water concentrations prevalent in the outermost interfacial layers.

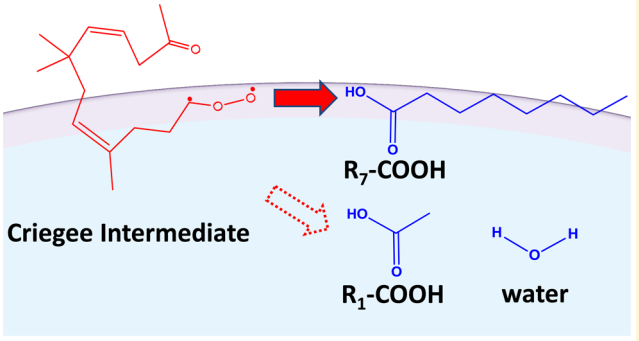

Criegee intermediates (CIs), the carbonyl oxides (R-CHOO) produced in the ozonation of unsaturated organic compounds, are deemed versatile oxidizers in the troposphere.[1−8] However, at the typical water vapor concentrations prevalent in the lower troposphere, which are orders of magnitude larger than those of most other species, measured rate constants of CIs' reactions with NO_2, SO_2, and H_2O in the gas phase[1,9−13] suggest that CIs will largely react with H_2O and water dimers $(H_2O)_2$.[14−22] These considerations raise the question of whether the CIs produced during reactions of unsaturated organics with $O_3(g)$ on the surface of aqueous aerosols will react exclusively with condensed H_2O therein. In contrast with extensive field,[7] modeling,[4] theoretical[6,14,20,23−26] and laboratory studies on CIs' chemistry in the gas phase,[3,16−19,22,27−30] there is no information on the chemistry of CIs at the air−water interface relevant to that taking place on fog droplets, aqueous aerosol, and thin water films.[14] It is perhaps redundant to emphasize the importance of multiphase chemistry in the lower troposphere after the severe haze-fog pollution episodes experienced over China megacities in recent years.[31−34]

The exothermic cycloaddition of ozone to olefins produces 1,2,3-trioxolanes (POZ*) possessing $E^* \approx 65$ kcal mol^{-1} excess internal energy.[2,35,36] In the gas phase, where collisional deactivation is competitive with chemically activated unimolecular processes,[20] POZ* largely decompose into even more excited ($E^* \approx 100$ kcal mol^{-1}) carbonyls and CIs.[35,37] Because vibrational energy relaxation in liquids is $\sim 10^3$ times faster than that in 1 atm of air, the ozonation of unsaturated species on aqueous surfaces could proceed along other mechanisms and generate different products than in the gas phase.[38,39] We have demonstrated that this is in fact the case in the ozonation of terpenes on water surfaces.[40]

Sesquiterpenes, such as α-humulene (α-H) and β-caryophyllene (β-C), are more powerful particle makers than isoprene or monoterpenes.[41,42] Recent experiments suggest that the reactive uptake of gaseous sesquiterpenes on mildly acidic water (bulk pH < 5) yields carbocations,[43] which could react with $O_3(g)$ therein to generate CIs at air−aqueous interfaces.[44] Recent calculations predict that the reaction of CH_2OO with water at the air−water interface takes place in a few picoseconds, which about 2−3 orders of magnitude faster than that in the gas phase, via interface-specific reaction pathways.[14] Experimental CIs' chemistry at aqueous interfaces, however, remains unexplored.

Herein, we report for the first time the detection of intermediates and products from reactions of CIs with H_2O, D_2O, $H_2{}^{18}O$, and carboxylic acids R_n-COOH (n = 1−7) on fresh surfaces of α-H or β-C solutions in acetonitrile (AN)/water (W) exposed to $O_3(g)$ for ~10 μs. We chose these sesquiterpenes as in situ sources of CIs because their high reactivity toward $O_3(g)$ is compatible with our pulse experiments, in which detectable amounts of products must be generated during the $\tau_R \approx 10$ μs contact times, that is, the lifetime of the intact microjets before they are fragmented by the nebulizer gas.[45−47] We chose an AN/W mixture solvent as a surrogate of atmospheric aqueous organic media because the composition of its interfacial layers is well characterized.[48−51]

Received: February 22, 2017
Accepted: March 20, 2017
Published: March 20, 2017

DOI: 10.1021/acs.jpclett.7b00434
J. Phys. Chem. Lett. 2017, 8, 1615−1623

Our experiments take place in the spraying chamber of the electrospray (ES) mass spectrometer that is continuously flushed with $O_3(g)/O_2(g)/N_2(g)$ mixtures at 1 atm and 298 K (see the Experimental Section and Figure S1 in the Supporting Information (SI)).[52,53]

Figure 1 shows negative ion ES mass spectra of the anions produced on the surface of microjets consisting of 1.0 mM α-H + 0.2 mM NaCl in AN/W (4:1 = vol:vol) solutions upon being exposed to $O_3(g)$ for $\tau_R \approx 10$ μs.

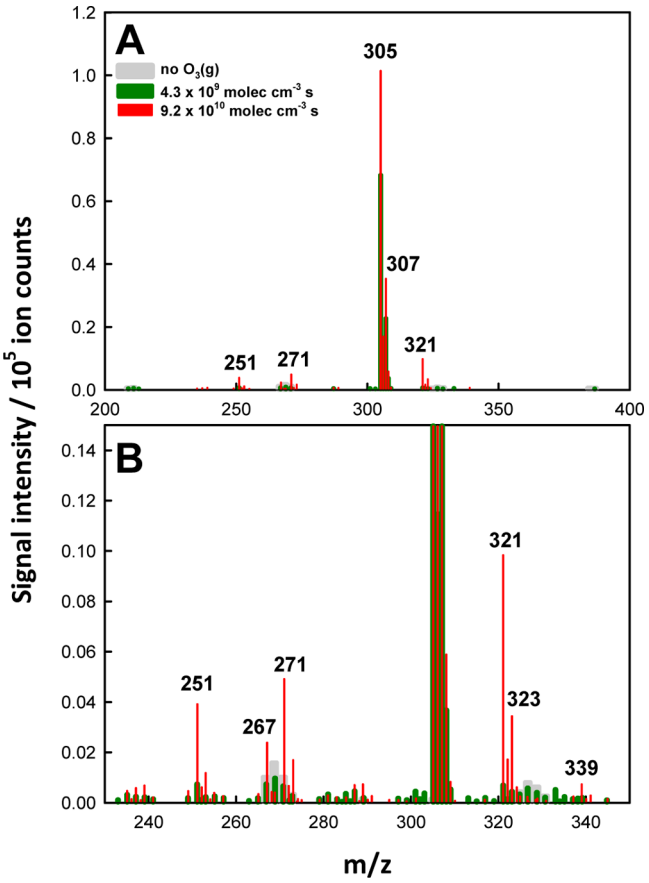

Figure 1. (A) Negative ion mass spectra from 1 mM α-H + 0.2 mM NaCl in AN/H_2O (4:1 = vol:vol) solution microjets in the absence (gray) and presence of $O_3(g)$ (green: $E = 4.3 \times 10^9$ molecules cm^{-3} s; red: $E = 9.2 \times 10^{10}$ molecules cm^{-3} s). (B) Zooming in on the ozonation products. The m/z 305 and 307 signals correspond to Cl^- adducts of α-hydroxy-hydroperoxides. See the text for details.

We have shown in a series of experiments from our laboratory that these ES mass spectra correspond to species generated by heterogeneous processes in the outermost interfacial layers of the microjets.[45,47,54,55] Such species are carried into the charged microdroplets generated by the nebulization of interfacial layers, which are ultimately ejected to the gas phase via a sequence of Coulomb explosions and detected within 1 ms.[56,57] The small ozone exposures, $E = [O_3(g)] \times \tau_R \leq 2.4 \times 10^{11}$ molecules cm^{-3} s, in present experiments enable us to monitor the very early stages of CI reactions on the liquid surface.

Our assignments are based on mass-specific signals. In the presence of Cl^-, the major negatively charged species detected in our experiments correspond to Cl^- adducts of neutrals, which are clearly identified by their characteristic $M/(M + 2) = 3/1$ ratio arising from the $^{35}Cl/^{37}Cl$ ratio of natural abundance Cl^-. We also detect smaller signals that correspond to the carboxylate anions derived from oxidation of the sesquiterpenes into acids under larger $O_3(g)$ exposures (Figure 1B, red). We verified that Cl^- is inert toward $O_3(g)$ under present conditions (Figure S2), as expected from $k_{O3+Cl-} < 0.003$ M^{-1} s^{-1} in bulk water[58] and our previous experiments.[59] AN is also inert; identical mass spectra were obtained in experiments using CH_3CN/H_2O and CD_3CN/H_2O solvent mixtures (Figure S3).

The most intense mass signals appear at $m/z = 305$ and 307 in a 305/307:3/1 ratio. They correspond to species resulting from the addition of O_3 (+48) to sesquiterpenes (MW = 204) C=C bonds, followed by H_2O addition (+18), which are detected as Cl^- adducts, namely, 305 (307) = 204 + 48 + 18 + 35 (37). Thus, the stoichiometry of 305/307 signals is consistent with hydroxy-hydroperoxides, produced from the addition of H_2O to ozonides or CIs produced in the reaction of O_3 to the sesquiterpenes (Scheme 1). The fact that neutral hydroxy-hydroperoxides are detected as Cl^- adducts is in accordance with literature reports on the strong affinity of Cl^- for related species.[29,60,61]

Other anion species formally arise from the addition of three ($m/z = 251 = 204 + 48 - 1$) and four ($m/z = 267 = 204 + 64 - 1$) O atoms to α-H, which must contain carboxylate anions, in addition to other functionalities (see Figure S4 for likely structures). The formation of carboxylates is in accordance with our previous study on the ozonolysis of β-C under similar conditions.[40] The $m/z = 321$ and 323 species, which contain five O atoms, are detected as the Cl^- adducts (see below). Similar (but not identical) spectra were obtained in the ozonolysis of β-C (Figure S5). Experiments in AN/D_2O (Figure 2) and AN/$H_2{}^{18}O$ (Figure S6) show that the m/z = 305/307 signals shift by +2 mass units into 307/309 signals in both cases, an observation that implies products involving the addition of one water molecule to α-H's CIs.

In contrast, the fact that the $m/z = 251$ signal shifts to m/z = 253 in AN/$H_2{}^{18}O$ (Figure S6) but not in AN/D_2O (Figure 2) is consistent with the presence of a carbonyl group that only exchanges an O atom with the solvent via its reversible hydration through a gem-diol, rather than with the addition of water. Note that the carbonyl functionality involved in the (ketone + $H_2O \leftrightarrow$ gem-diol) equilibrium, by lacking H atoms, can only exchange O atoms with the solvent. The opposite behavior is observed in the case of the $m/z = 321/323$ signals, which shift to 323/325 in AN/D_2O but remain unaltered in AN/$H_2{}^{18}O$. These findings exclude a water addition step in the genesis of $m/z = 321/323$ species and reveal the presence of two exchangeable hydrons, such as those of aldehydic −C(=O)H, alcohol −OH, and/or hydroperoxide −OOH groups (e.g., Figure S4). The functional groups carrying exchangeable hydrons are likely generated via CIs' further reactions with O_3.[23] The fact that neither $m/z = 251$ nor 267 signals shift in AN/D_2O implies they lack exchangeable hydrons. Therefore, on the basis of the analysis of experiments in $H_2{}^{18}O$, the m/z = 251 species must be keto-carboxylates $C_{15}H_{23}O_3^-$, whereas those at $m/z = 267$ are tentatively assigned to endoperoxy carboxylates $C_{15}H_{23}O_4^-$ (see Figure S4), which exchange neither D nor ^{18}O with water.[40] We had previously found endoperoxides in the interfacial ozonation of uric acid[62] and α-tocopherol.[53] Because the $m/z = 271/273$ signals shift by +4 units in both cases, as expected from products involving the addition of two water molecules, they could be assigned to C10 products with hydroxy-hydroperoxide groups at both ends (Figure S4). These experiments establish the stoichiometry and

DOI: 10.1021/acs.jpclett.7b00434
J. Phys. Chem. Lett. 2017, 8, 1615−1623

Scheme 1. Reaction Mechanism of α-H's CI at the Air–Liquid Interface

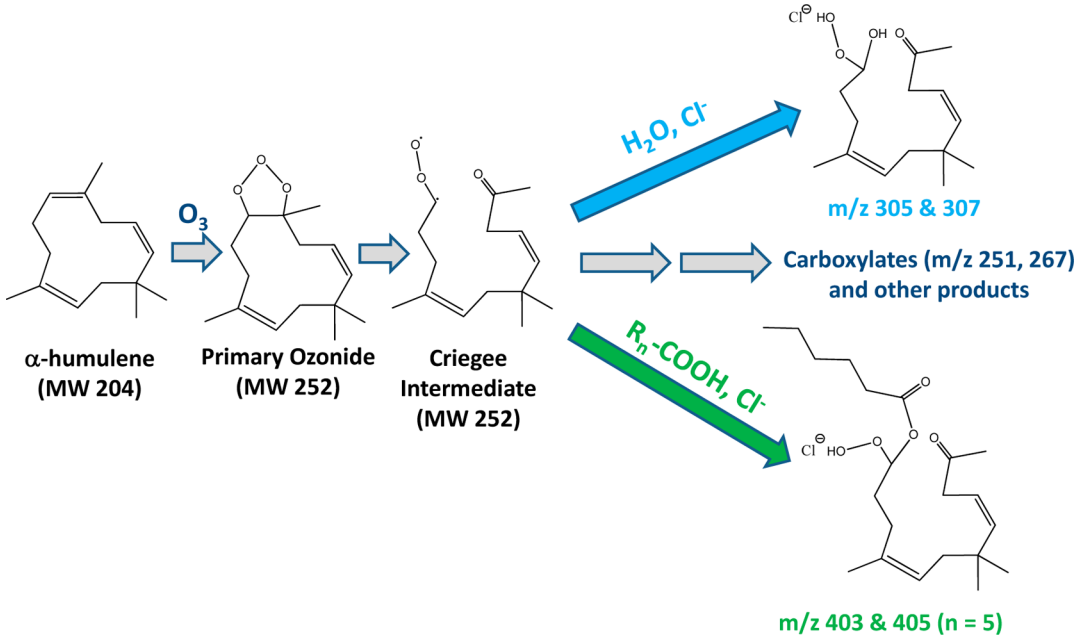

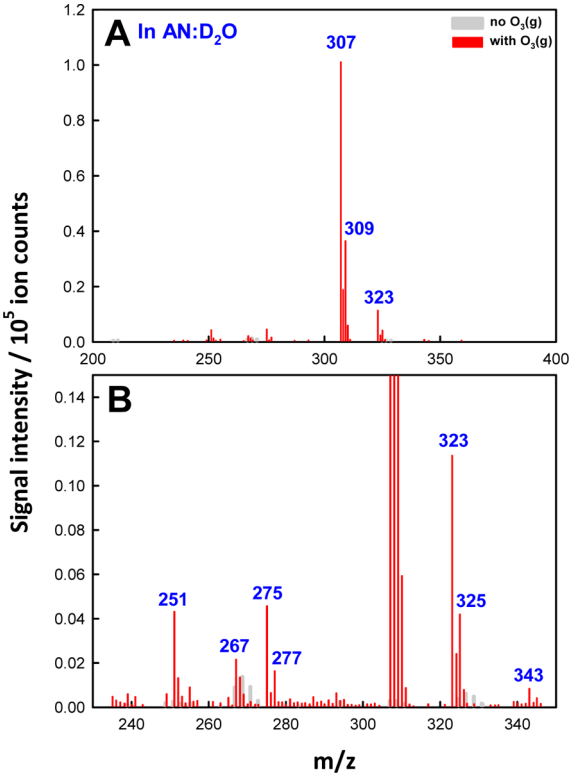

Figure 2. (A) Negative ion mass spectra from 1 mM α-H + 0.4 mM NaCl in AN/D_2O (4:1 = vol:vol) solution microjets in the absence (gray) and presence of O_3(g) (red, $E = 8.8 \times 10^{10}$ molecules cm^{-3} s). (B) Zooming in on the ozonation products.

functionality of products. However, in the absence of additional evidence, the presence of two (exo and endo) and three endo double bonds in β-C and α-H, respectively, leads to numerous possible isomers and prevents us from making more specific structural assignments. High-resolution MS/MS studies and theoretical calculations could help elucidate the molecular structures of the species detected in the present experiments.

These observations are consistent with the mechanism outlined in Scheme 1. α-H initially reacts with O_3 to form primary ozonides (POZ), which open up into carbonyl oxide structures, the CIs, which proceed into acids or react with water to produce R(−OH)(−OOH) (MW = 252 + 18 = 270) α-hydroxy-hydroperoxides. The presence of m/z = 287 (289) = 204 + 48 + 35 (37) signals in the ozonolysis of β-C (Figure S5) likely corresponds to relatively stable secondary ozonides (SOZ, Figure S4), rather than POZ or CI.[37] Because the gas-phase ozonolyses of α-H and β-C produce SOZ,[35,37] the absence of m/z 287 in the ozonolysis of α-H implies that the formation mechanism and reactivity of SOZ at the gas–liquid interface are different from those in the gas phase.[52,53,63,64]

OH radicals may not be involved in this chemistry because identical ES mass spectra were obtained in the absence and presence of amphiphilic isopropanol (IPA),[65,66] an efficient OH radical scavenger, $k_{OH+IPA} = 1.9 \times 10^9$ M^{-1} s^{-1} in bulk water and, most likely, also in W/AN mixtures (Figure 3).[67,68] Because OH radicals have been reported in ∼11% yields during gas-phase ozonolysis of α-H,[35] the lack of OH radical formation in our experiments suggests that fully stabilized CIs in collisions with the solvent would preferentially react with interfacial water rather than undergo the 1,4-hydrogen intramolecular transfer required to precede OH radical formation.[35]

The distinct evolution of different products as functions of O_3(g) exposure is shown in Figure 4. All signals display nonzero initial slopes except for that at m/z = 271. The largest m/z = 305/307 signals peak at $E \approx 3 \times 10^{10}$ molecules cm^{-3} s and decline afterward, which is consistent with further O_3 addition to remaining double bonds and/or unpaired electrons.[23] In contrast, signals at m/z = 251 and 267 increase with E to plateau above $E \approx 5 \times 10^{10}$ molecules cm^{-3} s. The second major m/z = 321/323 signals plateaus instead above $E \approx 2 \times 10^{11}$ molecules cm^{-3} s. The minor m/z = 271 signal is the only one that increases monotonically with E. The finite initial slopes of all signals, except that at m/z = 271, are consistent with the mechanism proposed in Scheme 1, in which the observed products are derived from a common CI primary

DOI: 10.1021/acs.jpclett.7b00434
J. Phys. Chem. Lett. 2017, 8, 1615–1623

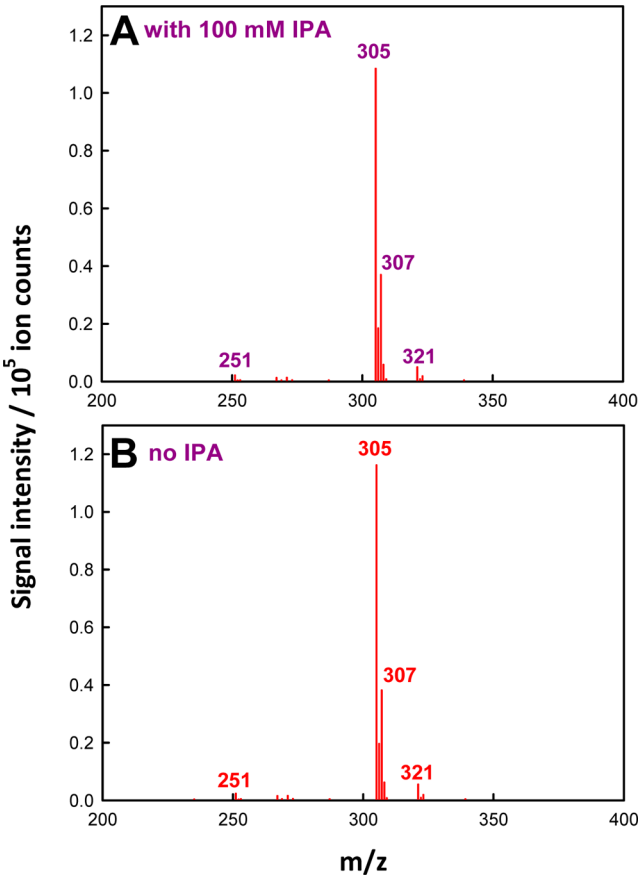

Figure 3. (A) Negative ion mass spectra from 1 mM α-H + 0.2 mM NaCl with 100 mM isopropanol (IPA) or (B) without IPA in AN/H_2O (4:1 = vol:vol) solution microjets in the presence of O_3(g) (E = 3.6 × 10^{10} molecules cm^{-3} s).

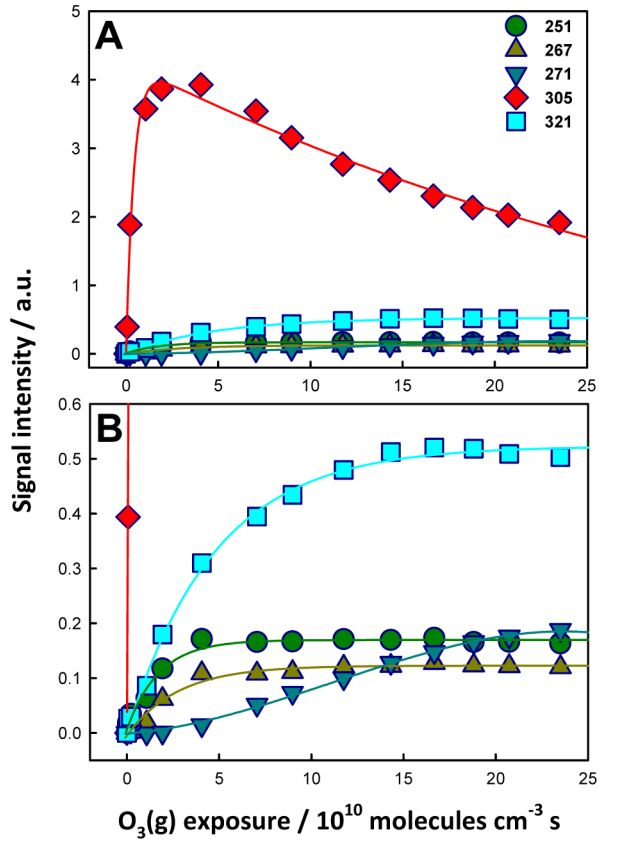

Figure 4. (A) Negative ion signal intensities of the products detected on 1 mM α-H + 0.2 mM NaCl in AN/H_2O (4:1 = vol:vol) solution microjets as a function of O_3(g) exposure. (B) Zoom-in plots. Connecting lines are guides to the eye. See the text for details.

intermediate. The decline of m/z = 305/307 signals above $E \approx$ 3 × 10^{10} molecules cm^{-3} s indicates that at larger O_3(g) exposures they are depleted faster than being formed. This observation implies that sesquiterpenes are depleted in the finite pool provided in the interfacial layers probed by our experiments.

Significantly, addition of R_n-COOH as cosolutes gives rise to new signals, X, which in the case of hexanoic acid (MW = 116) appear at m/z = 403/405 (Figure 5). We have previously shown that R_n-COOH/R_n-COO^- (n = 1−7) are inert toward O_3(g) under similar conditions.[55] The new (X) peaks in fact correspond to the products of R_5-COOH addition to CIs: 403 (405) = 204 + 48 + 116 + 35 (37). The distinct evolution of different products from 1 mM α-H + 0.2 mM NaCl + 100 mM R_5-COOH in AN/W (4:1 = vol:vol) solution microjets as a function of O_3(g) exposure is shown in Figure 6.

In our experiments, X signals are assigned to the products of R_n-COOH addition to sesquiterpene CIs at the gas−liquid interface (Scheme 1). A recent gas-phase kinetic study has shown that CH_2OO and CH_3CHOO react with formic and acetic acids in nearly every collision.[27] To our knowledge, our results are the first direct detection of reaction products from CIs + carboxylic acids at gas−aqueous interfaces. The competition between R_n-COOH and water at constant O_3 and R_n-COOH concentrations is expressed by the X/305 ratio. Figure 7 shows that the X/305 ratio is a strongly increasing function of n, which is consistent with the larger propensity of the longer alkyl chain acids for interfacial layers. The recently reported positive dependence of R_n-COO^-/R_n-COOH affinities for the air−water interface on chain length n accounts for the negligible X signals resulting from the addition of R_1-COOH (acetic acid) to CIs (see also Figures S7 and S8).[47,69−71] Together, these observations confirm that our experiments report processes taking place at the air−liquid interface rather than in the bulk liquids.

The above findings imply that 100 mM R_n-COOH compete with H_2O for CIs on the surface of AN/W mixtures that macroscopically are ~23 M (mf_{H2O} = 0.42) water. Because R_n-COOH and $(H_2O)_2$ are similarly reactive toward CIs in the gas phase,[11,19] it could have been expected that the fate of CIs at the interface would have been dictated by their exclusive reactions with H_2O. The fact that R_n-COOH effectively compete with H_2O for CIs implies that the gas−aqueous interface is a unique reaction medium, distinct from the gas or bulk water phases. The differences could be due to specific characteristics of water at interfacial layers, to the dissimilar affinities of H_2O and R_n-COOH for interfacial layers, or to a combination of both effects. A recent photoelectron microscopy study of AN/W liquid microjets showed that above mf_{AN} ≈ 0.2, the air−liquid interface consists of a nearly compact AN layer, which likely extends to the second layer.[48] Related molecular dynamics calculations of AN/W solutions qualified such a conclusion by revealing the "microheterogeneity" of outermost interfacial layers sparsely populated by disjoint water clusters.[49] It can be argued that molecules that are less polar and more hydrophobic than AN, such as those present in aqueous secondary organic aerosols, would be more enriched

DOI: 10.1021/acs.jpclett.7b00434
J. Phys. Chem. Lett. 2017, 8, 1615−1623

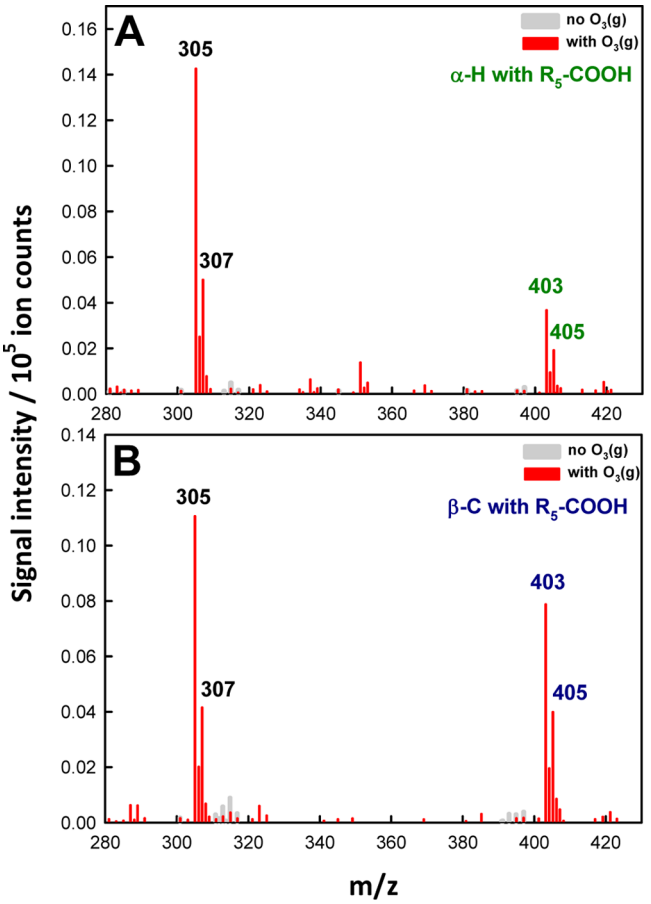

Figure 5. Negative ion mass spectra from 1 mM (A) α-H or (B) β-C + 0.2 mM NaCl + 100 mM hexanoic acid in AN/H_2O (4:1 = vol:vol) solution microjets in the absence (gray) and presence of O_3(g) (red, E = 2.4 × 10^{11} molecules cm^{-3} s).

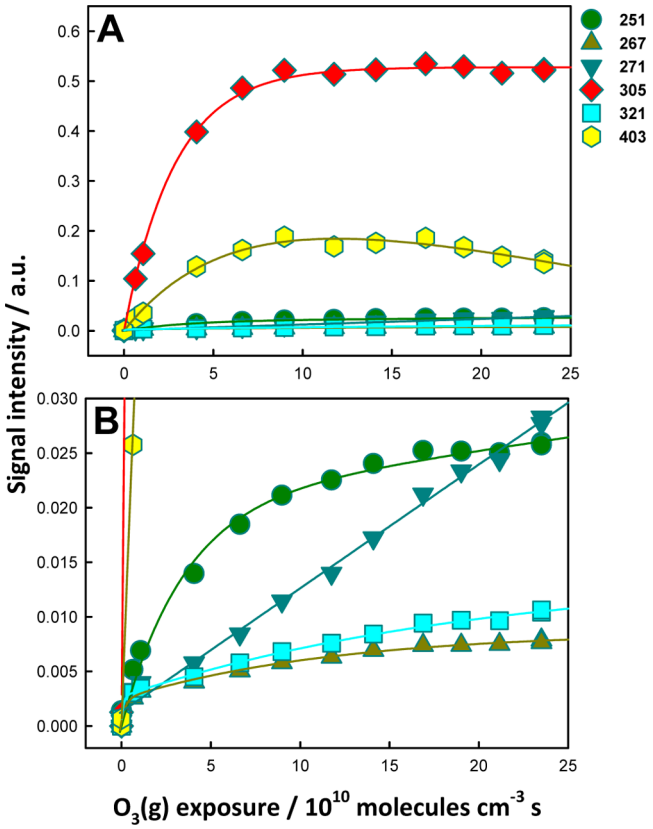

Figure 6. (A) Negative ion signal intensities of the products detected on 1 mM α-H + 0.2 mM NaCl + 100 mM hexanoic acid (R_5-COOH) in AN/H_2O (4:1 = vol:vol) solution microjets as a function of O_3(g) exposure. (B) Zoom-in plots. Connecting lines are guides to the eye.

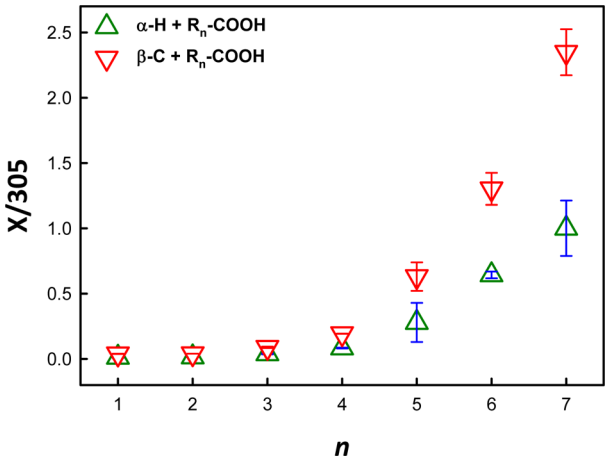

Figure 7. X/305 ratio of signal intensities from 1 mM α-H (up-triangles) or β-C (down-triangles) + 0.2 mM NaCl + 100 mM R_n-COOH (n = 1–7) in AN/H_2O (4:1 = vol:vol) microjets exposed to O_3(g) (E = 2.4 × 10^{11} molecules cm^{-3} s) as a function of n. X = 347, 361, 375, 389, 403, 417, and 431 for n = 1, 2, 3, 4, 5, 6, and 7, respectively. Error bars are derived from 2–6 independent measurements.

than AN in the interfacial layers.[72] A very recent VUV photoelectron spectroscopy study on the interfacial solvation of phenol and dihydroxybenzene in aqueous nanoaerosols supports such expectations.[73]

The mixing state and morphology of actual aqueous organic aerosols in the troposphere are therefore critical determinants of the reaction pathways open to CIs in interfacial layers.[74,75] Water and organics could be internally mixed or phase-separated into an aqueous core covered by an organic shell or in partially engulfed configurations,[74] depending on the functionality of organics, composition, temperature, relative humidity, and the presence of inorganic solutes. Our results show that even in the case of internally mixed solutions at the macroscopic scale, such as AN/W, concentration gradients naturally develop in the air–liquid interfacial layers where gas–liquid fast heterogeneous reactions take place. Reid et al., after carefully taking into account the interplay of various parameters, concluded that realistic aerosol particles under typical atmospheric conditions will adopt partially engulfed structures where organics coalesce into interfacial lenses, rather than the conceptually simpler aqueous core–organic shell configurations.[74] As indicated above, although our experiments could be thought to approach the core–shell morphology, the surface of the aqueous phase surrounding organic lenses in the partially engulfed structures will be preferentially populated by organics. Thus, we suggest that water concentrations at interfacial layers will be always smaller than those in the bulk phase. It is apparent that predicting the outcomes, rates, and products of interfacial reactions on aqueous organic aerosol is not straightforward.[8,76,77]

The present study simulates the reactions taking place on the surface of atmospheric aqueous aerosol matter exposed to O_3(g). O_3(g) will initially stick to the surface of aqueous

DOI: 10.1021/acs.jpclett.7b00434
J. Phys. Chem. Lett. 2017, 8, 1615–1623

organic aerosols to subsequently react with unsaturated organics therein to produce CIs in situ. It has been shown that unsaturated biogenic volatile organic compounds are protonated upon collision with acidic aqueous surfaces,[43,78−81] a phenomenon that enhances their uptake. The finding that CIs react with organics present on the surface of aerosol, rather than exclusively with water, leading to higher mass, less volatile products amounts to a process that promotes the stabilization of atmospheric particles.[82−84] Because in the case of sesquiterpenes the initial products (e.g., m/z 305 and X) still contain two (for α-H) and one (for β-C) C=C double bond(s), the atmospheric fate of such species will involve further oxidation by O_3(g). Note that both m/z 305 and X species also contain hydroperoxide −OOH groups, which can undergo thermal, metal-catalyzed, and photocatalyzed decompositions into OH radicals[85,86] or proceed to oligomerization.[28,29] These processes may be related to a recent report on the products of the ozonation of water infusions of ambient leaves, which revealed hitherto unidentified larger-mass organic species on leaf surfaces (m/z = 221, 305, 356, and 445).[44] By clarifying for the first time the mechanism of the interfacial ozonation of BVOCs in the outermost interfacial layers of atmospheric aqueous organic media, our results introduce unanticipated CI chemistry in atmospheric and forest environments.

It can be shown that the CIs produced in the gas phase will react mainly therein. This is borne out by the following considerations. Assuming a tropospheric environment at 30% relative humidity and 283 K ($[H_2O] = 1 \times 10^{17}$ molecules cm^{-3}, $[H_2O]_2/[H_2O]$ = WD/W $\approx 1 \times 10^{-3}$, WD $\approx 1 \times 10^{14}$ molecules cm^{-3}),[19] with $k_{CI+WD} = 1 \times 10^{-11}$ cm^3 molecule^{-1} s^{-1},[20] we get a pseudo-first-order rate constant for CI(g) decay via reaction with WD: $k_{-CI} = (1 \times 10^{-11}$ cm^3 molecule^{-1} s$^{-1}) \times 1 \times 10^{14}$ molecules cm$^{-3} = 1 \times 10^3$ s^{-1}. From an upper limit to the aqueous aerosol surface per unit volume of air in clear air, $S/V \approx 3 \times 10^{-5}$ cm^{-1},[87] and the expression given by the kinetic theory of gases for the frequency of CI collisions with aerosol surfaces, $k_{-aerosol} = 0.25\gamma c(S/V)$,[88] where $\gamma \approx 1$ is the uptake coefficient of CI(g) and $c \approx 3 \times 10^4$ cm s^{-1} is the mean thermal CI speed, we get $k_{-aerosol} \approx 0.23$ s^{-1}, that is, about 3 orders of magnitude smaller than the frequency of homogeneous CI losses in the gas phase, $k_{-CI} = 1 \times 10^3$ s^{-1}.

Summing up, our experiments probe for the first time the chemistry of CIs produced by ozonolysis of unsaturated compounds in the interfacial layers of model aqueous organic aerosols. We provided mass-specific identification and established the progeny of products and intermediates in a flash (<10 μs) reaction time frame. We found that CIs can react therein with amphiphilic carboxylic acids and more generally with similar OH-containing species, in competition with interfacial water molecules. Our findings point to unanticipated reaction pathways for CIs in the troposphere. Further work on this issue is underway.

EXPERIMENTAL SECTION

Our experiments involve the injection of sesquiterpene in AN/H_2O (4:1 = vol:vol) microjets into the spraying chamber of an electrospray mass spectrometer (ES-MS, Agilent 6130 quadrupole LC/MS electrospray system at NIES, Japan) flushed with N_2(g) at 1 atm and 298 K. Microjets are exposed therein to an orthogonal gas-phase O_3 beam (Figure S1). The species produced on the surface of such jets are analyzed in situ via online ES mass spectrometry. The present experimental setup is essentially the same as the one reported elsewhere.[54] Solutions are pumped (100 μL min^{-1}) into the spraying chamber through a grounded stainless steel needle (100 μm bore) coaxial with a sheath issuing nebulizer N_2(g) at a high gas velocity v_g (∼160 m/s). The species detected by ES mass spectrometry are produced in collisions of gaseous O_3 with the surface of the intact aqueous microjets as they emerge from the nozzle, that is, before they are broken up into submicrometer-sized droplets.[45,46] The modest polarizations of the initial microjets do not affect the observed phenomena.[53,89−92] Online mass-based sampling from the surface of continually refreshed aqueous microjets under ambient temperature and pressure makes our instrument a powerful surface-sensitive technique.[38,93] Further experimental details can be found in our previous publications.[46,54,90,91]

Ozone was generated by flowing ultrapure O_2(g) (>99.999%) through a silent discharge ozonizer (KSQ-050, Kotohira, Japan) and quantified via online UV−vis absorption spectrophotometry (Agilent 8453) at 250 and 300 nm [absorption cross sections σ(250 nm) = 1.1 × 10^{-17} and σ(300 nm) = 3.9 × 10^{-19} cm^2 molecule^{-1} at 298 K] prior to entering the reaction chamber. The reported [O_3(g)] values, which correspond to the concentrations actually sensed by the microjets in the reaction chamber, are estimated to be ∼12 times smaller than the values determined from UV absorbance due to further dilution by the drying nitrogen gas. Typical [O_3(g)] ranges from 6.4 × 10^{14} to 2.4 × 10^{16} molecules cm^{-3}.

Conditions in the present experiments were as follows: drying nitrogen gas flow rate: 12 L min^{-1}; drying nitrogen gas temperature: 340 °C; inlet voltage: +3.5 kV relative to ground; fragmentor voltage value: 60. All solutions were prepared in purified water (resistivity ≥ 18.2 M cm at 298 K) from a Millipore Milli-Q water purification system. All data were confirmed by at least duplicate experiments.

Chemicals: α-H (≥96.0%, Sigma-Aldrich), β-C (≥98.5%, Sigma-Aldrich), AN (≥99.8% for LC/MS, Wako), D_2O (>99.9 atom % D, Sigma-Aldrich), $H_2{}^{18}O$ (97%, Santa Cruz Isotope), 2-propanol (JP grade, Wako), AN-d_3 (CD_3CN, 99.8 atom % D, Sigma-Aldrich), acetic acid (>99.5%, WAKO), propionic acid (>98%, WAKO), butyric acid (>98%, WAKO), pentanoic acid (>95%, WAKO), hexanoic acid (>99%, WAKO), heptanoic acid (>98%, WAKO), octanoic acid (>97%, WAKO), and NaCl (≥99.999%, Sigma-Aldrich) were used as received.

ASSOCIATED CONTENT

Supporting Information

The Supporting Information is available free of charge on the ACS Publications website at DOI: 10.1021/acs.jpclett.7b00434.

Schematic diagram of the present experimental setup, possible structures of products, and additional data (PDF)

AUTHOR INFORMATION

Corresponding Authors

*E-mail: enami.shinichi@nies.go.jp. Phone: +81-29-850-2770 (S.E.).

*E-mail: ajcoluss@caltech.edu. Phone: +1-626-395-6350 (A.J.C.).

ORCID

Shinichi Enami: 0000-0002-2790-7361

DOI: 10.1021/acs.jpclett.7b00434
J. Phys. Chem. Lett. 2017, 8, 1615−1623

Author Contributions

S.E. designed and performed research; S.E. and A.J.C. analyzed data and wrote the paper.

Notes

The authors declare no competing financial interest.

■ ACKNOWLEDGMENTS

We are grateful to Drs. Satoshi Inomata, Akihiro Fushimi, and Kei Sato of NIES, Prof. Yosuke Sakamoto of Kyoto University, and Prof. Jun Hirokawa of Hokkaido University for helpful discussion. S.E. is grateful to the Research Foundation for Opto-science and Technology, JSPS KAKENHI Grant Numbers 15H05328 and 15K12188.

■ REFERENCES

(1) Lee, Y. P. Perspective: Spectroscopy and Kinetics of Small Gaseous Criegee Intermediates. *J. Chem. Phys.* **2015**, *143*, 020901.
(2) Criegee, R. Mechanism of Ozonolysis. *Angew. Chem., Int. Ed. Engl.* **1975**, *14*, 745−752.
(3) Nguyen, T. B.; et al. Atmospheric Fates of Criegee Intermediates in the Ozonolysis of Isoprene. *Phys. Chem. Chem. Phys.* **2016**, *18*, 10241−10254.
(4) Taatjes, C. A.; Shallcross, D. E.; Percival, C. J. Research Frontiers in the Chemistry of Criegee Intermediates and Tropospheric Ozonolysis. *Phys. Chem. Chem. Phys.* **2014**, *16*, 1704−1718.
(5) Welz, O.; Savee, J. D.; Osborn, D. L.; Vasu, S. S.; Percival, C. J.; Shallcross, D. E.; Taatjes, C. A. Direct Kinetic Measurements of Criegee Intermediate (CH_2OO) Formed by Reaction of CH_2I with O_2. *Science* **2012**, *335*, 204−207.
(6) Vereecken, L.; Harder, H.; Novelli, A. The Reaction of Criegee Intermediates with NO, RO_2, and SO_2, and Their Fate in the Atmosphere. *Phys. Chem. Chem. Phys.* **2012**, *14*, 14682−14695.
(7) Mauldin, R. L., III; Berndt, T.; Sipila, M.; Paasonen, P.; Petaja, T.; Kim, S.; Kurten, T.; Stratmann, F.; Kerminen, V. M.; Kulmala, M. A New Atmospherically Relevant Oxidant of Sulphur Dioxide. *Nature* **2012**, *488*, 193−196.
(8) Riva, M.; Budisulistiorini, S. H.; Zhang, Z.; Gold, A.; Thornton, J. A.; Turpin, B. J.; Surratt, J. D. Multiphase Reactivity of Gaseous Hydroperoxide Oligomers Produced from Isoprene Ozonolysis in the Presence of Acidified Aerosols. *Atmos. Environ.* **2017**, *152*, 314−322.
(9) Kidwell, N. M.; Li, H. W.; Wang, X. H.; Bowman, J. M.; Lester, M. I. Unimolecular Dissociation Dynamics of Vibrationally Activated CH_3CHOO Criegee Intermediates to OH Radical Products. *Nat. Chem.* **2016**, *8*, 509−514.
(10) Stone, D.; Whalley, L. K.; Heard, D. E. Tropospheric OH and HO_2 Radicals: Field Measurements and Model Comparisons. *Chem. Soc. Rev.* **2012**, *41*, 6348−6404.
(11) Osborn, D. L.; Taatjes, C. A. The Physical Chemistry of Criegee Intermediates in the Gas Phase. *Int. Rev. Phys. Chem.* **2015**, *34*, 309−360.
(12) Stone, D.; Blitz, M.; Daubney, L.; Howes, N. U. M.; Seakins, P. Kinetics of CH_2OO Reactions with SO_2, NO_2, NO, H_2O and CH_3CHO as a Function of Pressure. *Phys. Chem. Chem. Phys.* **2014**, *16*, 1139−1149.
(13) Newland, M. J.; Rickard, A. R.; Alam, M. S.; Vereecken, L.; Munoz, A.; Rodenas, M.; Bloss, W. J. Kinetics of Stabilised Criegee Intermediates Derived from Alkene Ozonolysis: Reactions with SO_2, H_2O and Decomposition under Boundary Layer Conditions. *Phys. Chem. Chem. Phys.* **2015**, *17*, 4076−4088.
(14) Zhu, C. Q.; Kumar, M.; Zhong, J.; Li, L.; Francisco, J. S.; Zeng, X. C. New Mechanistic Pathways for Criegee-Water Chemistry at the Air/Water Interface. *J. Am. Chem. Soc.* **2016**, *138*, 11164−11169.
(15) Berndt, T.; Voigtlander, J.; Stratmann, F.; Junninen, H.; Mauldin, R. L., III; Sipila, M.; Kulmala, M.; Herrmann, H. Competing Atmospheric Reactions of CH_2OO with SO_2 and Water Vapour. *Phys. Chem. Chem. Phys.* **2014**, *16*, 19130−19136.
(16) Chao, W.; Hsieh, J. T.; Chang, C. H.; Lin, J. J. M. Direct Kinetic Measurement of the Reaction of the Simplest Criegee Intermediate with Water Vapor. *Science* **2015**, *347*, 751−754.
(17) Huang, H. L.; Chao, W.; Lin, J. J. M. Kinetics of a Criegee Intermediate That Would Survive High Humidity and May Oxidize Atmospheric SO_2. *Proc. Natl. Acad. Sci. U. S. A.* **2015**, *112*, 10857−10862.
(18) Lewis, T. R.; Blitz, M. A.; Heard, D. E.; Seakins, P. W. Direct Evidence for a Substantive Reaction between the Criegee Intermediate, CH_2OO, and the Water Vapour Dimer. *Phys. Chem. Chem. Phys.* **2015**, *17*, 4859−4863.
(19) Lin, L. C.; Chang, H. T.; Chang, C. H.; Chao, W.; Smith, M. C.; Chang, C. H.; Lin, J. J. M.; Takahashi, K. Competition between H_2O and $(H_2O)_2$ Reactions with CH_2OO/CH_3CHOO. *Phys. Chem. Chem. Phys.* **2016**, *18*, 4557−4568.
(20) Long, B.; Bao, J. L.; Truhlar, D. G. Atmospheric Chemistry of Criegee Intermediates: Unimolecular Reactions and Reactions with Water. *J. Am. Chem. Soc.* **2016**, *138*, 14409−14422.
(21) Anglada, J. M.; Sole, A. Impact of the Water Dimer on the Atmospheric Reactivity of Carbonyl Oxides. *Phys. Chem. Chem. Phys.* **2016**, *18*, 17698−17712.
(22) Smith, M. C.; Chang, C. H.; Chao, W.; Lin, L. C.; Takahashi, K.; Boering, K. A.; Lin, J. J. M. Strong Negative Temperature Dependence of the Simplest Criegee Intermediate CH_2OO Reaction with Water Dimer. *J. Phys. Chem. Lett.* **2015**, *6*, 2708−2713.
(23) Kjaergaard, H. G.; Kurten, T.; Nielsen, L. B.; Jorgensen, S.; Wennberg, P. O. Criegee Intermediates React with Ozone. *J. Phys. Chem. Lett.* **2013**, *4*, 2525−2529.
(24) Vereecken, L.; Harder, H.; Novelli, A. The Reactions of Criegee Intermediates with Alkenes, Ozone, and Carbonyl Oxides. *Phys. Chem. Chem. Phys.* **2014**, *16*, 4039−4049.
(25) Vereecken, L.; Rickard, A. R.; Newland, M. J.; Bloss, W. J. Theoretical Study of the Reactions of Criegee Intermediates with Ozone, Alkylhydroperoxides, and Carbon Monoxide. *Phys. Chem. Chem. Phys.* **2015**, *17*, 23847−23858.
(26) Aplincourt, P.; Anglada, J. M. Theoretical Studies of the Isoprene Ozonolysis under Tropospheric Conditions. 2. Unimolecular and Water-Assisted Decomposition of the alpha-Hydroxy Hydroperoxides. *J. Phys. Chem. A* **2003**, *107*, 5812−5820.
(27) Welz, O.; et al. Rate Coefficients of C1 and C2 Criegee Intermediate Reactions with Formic and Acetic Acid near the Collision Limit: Direct Kinetics Measurements and Atmospheric Implications. *Angew. Chem., Int. Ed.* **2014**, *53*, 4547−4550.
(28) Sakamoto, Y.; Yajima, R.; Inomata, S.; Hirokawa, J. Water Vapour Effects on Secondary Organic Aerosol Formation in Isoprene Ozonolysis. *Phys. Chem. Chem. Phys.* **2017**, *19*, 3165−3175.
(29) Sakamoto, Y.; Inomata, S.; Hirokawa, J. Oligomerization Reaction of the Criegee Intermediate Leads to Secondary Organic Aerosol Formation in Ethylene Ozonolysis. *J. Phys. Chem. A* **2013**, *117*, 12912−12921.
(30) Hatakeyama, S.; Akimoto, H. Reactions of Criegee Intermediates in the Gas-Phase. *Res. Chem. Intermed.* **1994**, *20*, 503−524.
(31) Fu, H.; Chen, J. Formation, Features and Controlling Strategies of Severe Haze-Fog Pollutions in China. *Sci. Total Environ.* **2017**, *578*, 121−138.
(32) Zheng, G.; Duan, F.; Su, H.; Ma, Y.; Cheng, Y.; Zheng, B.; Zhang, Q.; Huang, T.; Kimoto, T.; Chang, D.; et al. Exploring the Severe Winter Haze in Beijing: The Impact of Synoptic Weather, Regional Transport and Heterogeneous Reactions. *Atmos. Chem. Phys.* **2015**, *15*, 2969−2983.
(33) Kulmala, M. China's Choking Cocktail. *Nature* **2015**, *526*, 497.
(34) Cheng, Y.; Zheng, G.; Wei, C.; Mu, Q.; Zheng, B.; Wang, Z.; Gao, M.; Zhang, Q.; He, K.; Carmichael, G.; et al. Reactive Nitrogen Chemistry in Aerosol Water as a Source of Sulfate During Haze Events in China. *Sci. Adv.* **2016**, *2*, e1601530.
(35) Beck, M.; Winterhalter, R.; Herrmann, F.; Moortgat, G. K. The Gas-Phase Ozonolysis of Alpha-Humulene. *Phys. Chem. Chem. Phys.* **2011**, *13*, 10970−11001.

DOI: 10.1021/acs.jpclett.7b00434
J. Phys. Chem. Lett. 2017, 8, 1615−1623

(36) Chuong, B.; Zhang, J.; Donahue, N. M. Cycloalkene Ozonolysis: Collisionally Mediated Mechanistic Branching. *J. Am. Chem. Soc.* **2004**, *126*, 12363−12373.
(37) Winterhalter, R.; Herrmann, F.; Kanawati, B.; Nguyen, T. L.; Peeters, J.; Vereecken, L.; Moortgat, G. K. The Gas-Phase Ozonolysis of Beta-Caryophyllene ($C_{15}H_{24}$). Part I: An Experimental Study. *Phys. Chem. Chem. Phys.* **2009**, *11*, 4152−4172.
(38) Chapleski, R. C.; Zhang, Y.; Troya, D.; Morris, J. R. Heterogeneous Chemistry and Reaction Dynamics of the Atmospheric Oxidants, O_3, NO_3, and OH, on Organic Surfaces. *Chem. Soc. Rev.* **2016**, *45*, 3731−3746.
(39) Finlayson-Pitts, B. J. Reactions at Surfaces in the Atmosphere: Integration of Experiments and Theory as Necessary (but Not Necessarily Sufficient) for Predicting the Physical Chemistry of Aerosols. *Phys. Chem. Chem. Phys.* **2009**, *11*, 7760−7779.
(40) Enami, S.; Hoffmann, M. R.; Colussi, A. J. Prompt Formation of Organic Acids in Pulse Ozonation of Terpenes on Aqueous Surfaces. *J. Phys. Chem. Lett.* **2010**, *1*, 2374−2379.
(41) Chan, A. W. H.; et al. Speciated Measurements of Semivolatile and Intermediate Volatility Organic Compounds (S/IVOCs) in a Pine Forest During BEACHON-RoMBAS 2011. *Atmos. Chem. Phys.* **2016**, *16*, 1187−1205.
(42) Yao, L.; Ma, Y.; Wang, L.; Zheng, J.; Khalizov, A.; Chen, M. D.; Zhou, Y. Y.; Qi, L.; Cui, F. P. Role of Stabilized Criegee Intermediate in Secondary Organic Aerosol Formation from the Ozonolysis of Alpha-Cedrene. *Atmos. Environ.* **2014**, *94*, 448−457.
(43) Matsuoka, K.; Sakamoto, Y.; Hama, T.; Kajii, Y.; Enami, S. Reactive Uptake of Gaseous Sesquiterpenes on Aqueous Surfaces. *J. Phys. Chem. A* **2017**, *121*, 810−818.
(44) Potier, E.; Loubet, B.; Durand, B.; Flura, D.; Bourdat-Deschamps, M.; Ciuraru, R.; Ogée, J. Chemical Reaction Rates of Ozone in Water Infusions of Wheat, Beech, Oak and Pine Leaves of Different Ages. *Atmos. Environ.* **2017**, *151*, 176−187.
(45) Enami, S.; Colussi, A. J. Long-Range Hofmeister Effects of Anionic and Cationic Amphiphiles. *J. Phys. Chem. B* **2013**, *117*, 6276−6281.
(46) Enami, S.; Colussi, A. J. Long-Range Specific Ion-Ion Interactions in Hydrogen-Bonded Liquid Films. *J. Chem. Phys.* **2013**, *138*, 184706.
(47) Enami, S.; Fujii, T.; Sakamoto, Y.; Hama, T.; Kajii, Y. Carboxylate Ion Availability at the Air-Water Interface. *J. Phys. Chem. A* **2016**, *120*, 9224−9234.
(48) Perrine, K. A.; Van Spyk, M. H.; Margarella, A. M.; Winter, B.; Faubel, M.; Bluhm, H.; Hemminger, J. C. Characterization of the Acetonitrile Aqueous Solution/Vapor Interface by Liquid-Jet X-Ray Photoelectron Spectroscopy. *J. Phys. Chem. C* **2014**, *118*, 29378−29388.
(49) Makowski, M. J.; Stern, A. C.; Hemminger, J. C.; Tobias, D. J. Orientation and Structure of Acetonitrile in Water at the Liquid−Vapor Interface: A Molecular Dynamics Simulation Study. *J. Phys. Chem. C* **2016**, *120*, 17555−17563.
(50) Rao, Y.; Turro, N. J.; Eisenthal, K. B. Water Structure at Air/Acetonitrile Aqueous Solution Interfaces. *J. Phys. Chem. C* **2009**, *113*, 14384−14389.
(51) Paul, S.; Chandra, A. Liquid-Vapor Interfaces of Water-Acetonitrile Mixtures of Varying Composition. *J. Chem. Phys.* **2005**, *123*, 184706.
(52) Enami, S.; Hoffmann, M. R.; Colussi, A. J. Acidity Enhances the Formation of a Persistent Ozonide at Aqueous Ascorbate/Ozone Gas Interfaces. *Proc. Natl. Acad. Sci. U. S. A.* **2008**, *105*, 7365−7369.
(53) Enami, S.; Hoffmann, M. R.; Colussi, A. J. How Phenol and Alpha-Tocopherol React with Ambient Ozone at Gas/Liquid Interfaces. *J. Phys. Chem. A* **2009**, *113*, 7002−7010.
(54) Enami, S.; Sakamoto, Y.; Colussi, A. J. Fenton Chemistry at Aqueous Interfaces. *Proc. Natl. Acad. Sci. U. S. A.* **2014**, *111*, 623−628.
(55) Enami, S.; Hoffmann, M. R.; Colussi, A. J. In Situ Mass Spectrometric Detection of Interfacial Intermediates in the Oxidation of RCOOH(aq) by Gas-Phase OH-Radicals. *J. Phys. Chem. A* **2014**, *118*, 4130−4137.
(56) Nguyen, S.; Fenn, J. B. Gas-Phase Ions of Solute Species from Charged Droplets of Solutions. *Proc. Natl. Acad. Sci. U. S. A.* **2007**, *104*, 1111−1117.
(57) Kebarle, P.; Peschke, M. On the Mechanisms by Which the Charged Droplets Produced by Electrospray Lead to Gas Phase Ions. *Anal. Chim. Acta* **2000**, *406*, 11−35.
(58) Hoigne, J.; Bader, H.; Haag, W. R.; Staehelin, J. Rate Constants of Reactions of Ozone with Organic and Inorganic-Compounds in Water-III. Inorganic-Compounds and Radicals. *Water Res.* **1985**, *19*, 993−1004.
(59) Enami, S.; Vecitis, C. D.; Cheng, J.; Hoffmann, M. R.; Colussi, A. J. Global Inorganic Source of Atmospheric Bromine. *J. Phys. Chem. A* **2007**, *111*, 8749−8752.
(60) Larson, J. W.; McMahon, T. B. Fluoride and Chloride Affinities of Main Group Oxides, Fluorides, Oxofluorides, and Alkyls. Quantitative Scales of Lewis Acidities from Ion Cyclotron Resonance Halide-Exchange Equilibria. *J. Am. Chem. Soc.* **1985**, *107*, 766−773.
(61) Bohringer, H.; Fahey, D. W.; Fehsenfeld, F. C.; Ferguson, E. E. Bond-Energies of the Molecules H_2O, SO_2, H_2O_2, and HCl to Various Atmospheric Negative-Ions. *J. Chem. Phys.* **1984**, *81*, 2805−2810.
(62) Enami, S.; Hoffmann, A. R.; Colussi, A. J. Ozonolysis of Uric Acid at the Air/Water Interface. *J. Phys. Chem. B* **2008**, *112*, 4153−4156.
(63) Thompson, K. C.; et al. Reaction of a Phospholipid Monolayer with Gas-Phase Ozone at the Air-Water Interface: Measurement of Surface Excess and Surface Pressure in Real Time. *Langmuir* **2010**, *26*, 17295−17303.
(64) Karagulian, F.; Lea, A. S.; Dilbeck, C. W.; Finlayson-Pitts, B. J. A New Mechanism for Ozonolysis of Unsaturated Organics on Solids: Phosphocholines on NaCl as a Model for Sea Salt Particles. *Phys. Chem. Chem. Phys.* **2008**, *10*, 528−541.
(65) Kataoka, S.; Cremer, P. S. Probing Molecular Structure at Interfaces for Comparison with Bulk Solution Behavior: Water/2-Propanol Mixtures Monitored by Vibrational Sum Frequency Spectroscopy. *J. Am. Chem. Soc.* **2006**, *128*, 5516−5522.
(66) Vazquez, G.; Alvarez, E.; Navaza, J. M. Surface Tension of Alcohol + Water from 20 to 50 C. *J. Chem. Eng. Data* **1995**, *40*, 611−614.
(67) Buxton, G. V.; Greenstock, C. L.; Helman, W. P.; Ross, A. B. Critical-Review of Rate Constants for Reactions of Hydrated Electrons, Hydrogen-Atoms and Hydroxyl Radicals ($\cdot$OH/$\cdot O^-$) in Aqueous-Solution. *J. Phys. Chem. Ref. Data* **1988**, *17*, 513−886.
(68) Brizzolari, A.; Campisi, G. M.; Santaniello, E.; Razzaghi-Asl, N.; Saso, L.; Foti, M. C. Effect of Organic Co-Solvents in the Evaluation of the Hydroxyl Radical Scavenging Activity by the 2-Deoxyribose Degradation Assay: The Paradigmatic Case of Alpha-Lipoic Acid. *Biophys. Chem.* **2017**, *220*, 1−6.
(69) Lee, M. T.; Orlando, F.; Artiglia, L.; Chen, S. Z.; Ammann, M. Chemical Composition and Properties of the Liquid-Vapor Interface of Aqueous C1 to C4 Monofunctional Acid and Alcohol Solutions. *J. Phys. Chem. A* **2016**, *120*, 9749−9758.
(70) Ottosson, N.; Wernersson, E.; Soderstrom, J.; Pokapanich, W.; Kaufmann, S.; Svensson, S.; Persson, I.; Ohrwall, G.; Bjorneholm, O. The Protonation State of Small Carboxylic Acids at the Water Surface from Photoelectron Spectroscopy. *Phys. Chem. Chem. Phys.* **2011**, *13*, 12261−12267.
(71) Hayase, S.; Yabushita, A.; Kawasaki, M.; Enami, S.; Hoffmann, M. R.; Colussi, A. J. Weak Acids Enhance Halogen Activation on Atmospheric Water's Surfaces. *J. Phys. Chem. A* **2011**, *115*, 4935−4940.
(72) Donaldson, D. J.; Valsaraj, K. T. Adsorption and Reaction of Trace Gas-Phase Organic Compounds on Atmospheric Water Film Surfaces: A Critical Review. *Environ. Sci. Technol.* **2010**, *44*, 865−873.
(73) Lin, P. C.; Wu, Z. H.; Chen, M. S.; Li, Y. L.; Chen, W. R.; Huang, T. P.; Lee, Y. Y.; Wang, C. C. Interfacial Solvation and Surface pH of Phenol and Dihydroxybenzene Aqueous Nanoaerosols Unveiled by Aerosol VUV Photoelectron Spectroscopy. *J. Phys. Chem. B* **2017**, *121*, 1054−1067.
(74) Reid, J. P.; Dennis-Smither, B. J.; Kwamena, N.O. A.; Miles, R. E.; Hanford, K. L.; Homer, C. J. The Morphology of Aerosol Particles

DOI: 10.1021/acs.jpclett.7b00434
J. Phys. Chem. Lett. 2017, 8, 1615−1623

Consisting of Hydrophobic and Hydrophilic Phases: Hydrocarbons, Alcohols and Fatty Acids as the Hydrophobic Component. *Phys. Chem. Chem. Phys.* **2011**, *13*, 15559−15572.
(75) Pye, H. O.; Murphy, B. N.; Xu, L.; Ng, N. L.; Carlton, A. G.; Guo, H.; Weber, R.; Vasilakos, P.; Appel, K. W.; Budisulistiorini, S. H.; et al. On the Implications of Aerosol Liquid Water and Phase Separation for Organic Aerosol Mass. *Atmos. Chem. Phys.* **2017**, *17*, 343−369.
(76) Faust, J. A.; Wong, J. P.; Lee, A. K.; Abbatt, J. P. Role of Aerosol Liquid Water in Secondary Organic Aerosol Formation from Volatile Organic Compounds. *Environ. Sci. Technol.* **2017**, *51*, 1405−1413.
(77) Marsh, A.; Rovelli, G.; Song, Y. C.; Pereira, K. L.; Willoughby, R. E.; Bzdek, B. R.; Hamilton, J.; Orr-Ewing, A.; Topping, D. O.; Reid, J. P. Accurate Representations of the Physicochemical Properties of Atmospheric Aerosols: When Are Laboratory Measurements of Value? *Faraday Discuss.* **2017**, DOI: 10.1039/C7FD00008A.
(78) Enami, S.; Mishra, H.; Hoffmann, M. R.; Colussi, A. J. Protonation and Oligomerization of Gaseous Isoprene on Mildly Acidic Surfaces: Implications for Atmospheric Chemistry. *J. Phys. Chem. A* **2012**, *116*, 6027−6032.
(79) Enami, S.; Hoffmann, M. R.; Colussi, A. J. Dry Deposition of Biogenic Terpenes Via Cationic Oligomerization on Environmental Aqueous Surfaces. *J. Phys. Chem. Lett.* **2012**, *3*, 3102−3108.
(80) Liggio, J.; Li, S. M.; Brook, J. R.; Mihele, C. Direct Polymerization of Isoprene and Alpha-Pinene on Acidic Aerosols. *Geophys. Res. Lett.* **2007**, DOI: 10.1029/2006GL028468.
(81) Connelly, B. M.; Tolbert, M. A. Reaction of Isoprene on Thin Sulfuric Acid Films: Kinetics, Uptake, and Product Analysis. *Environ. Sci. Technol.* **2010**, *44*, 4603−4608.
(82) Zhao, Y.; Wingen, L. M.; Perraud, V.; Finlayson-Pitts, B. J. Phase, Composition, and Growth Mechanism for Secondary Organic Aerosol from the Ozonolysis of Alpha-Cedrene. *Atmos. Chem. Phys.* **2016**, *16*, 3245−3264.
(83) Riccobono, F.; et al. Oxidation Products of Biogenic Emissions Contribute to Nucleation of Atmospheric Particles. *Science* **2014**, *344*, 717−721.
(84) Virtanen, A.; et al. An Amorphous Solid State of Biogenic Secondary Organic Aerosol Particles. *Nature* **2010**, *467*, 824−827.
(85) Tong, H.; Arangio, A. M.; Lakey, P. S. J.; Berkemeier, T.; Liu, F.; Kampf, C. J.; Brune, W. H.; Pöschl, U.; Shiraiwa, M. Hydroxyl Radicals from Secondary Organic Aerosol Decomposition in Water. *Atmos. Chem. Phys.* **2016**, *16*, 1761−1771.
(86) Vidrio, E.; Phuah, C. H.; Dillner, A. M.; Anastasio, C. Generation of Hydroxyl Radicals from Ambient Fine Particles in a Surrogate Lung Fluid Solution. *Environ. Sci. Technol.* **2009**, *43*, 922−927.
(87) Reisinger, A. R. Observations of HNO_2 in the Polluted Winter Atmosphere: Possible Heterogeneous Production on Aerosols. *Atmos. Environ.* **2000**, *34*, 3865−3874.
(88) Davidovits, P.; Kolb, C. E.; Williams, L. R.; Jayne, J. T.; Worsnop, D. R. Update 1 of: Mass Accommodation and Chemical Reactions at Gas-Liquid Interfaces. *Chem. Rev.* **2011**, *111*, PR76−PR109.
(89) Mishra, H.; Enami, S.; Nielsen, R. J.; Stewart, L. A.; Hoffmann, M. R.; Goddard, W. A.; Colussi, A. J. Brønsted Basicity of the Air-Water Interface. *Proc. Natl. Acad. Sci. U. S. A.* **2012**, *109*, 18679−18683.
(90) Enami, S.; Hoffmann, M. R.; Colussi, A. J. Molecular Control of Reactive Gas Uptake "on Water". *J. Phys. Chem. A* **2010**, *114*, 5817−5822.
(91) Enami, S.; Hoffmann, M. R.; Colussi, A. J. Proton Availability at the Air/Water Interface. *J. Phys. Chem. Lett.* **2010**, *1*, 1599−1604.
(92) Enami, S.; Vecitis, C. D.; Cheng, J.; Hoffmann, M. R.; Colussi, A. J. Electrospray Mass Spectrometric Detection of Products and Short-Lived Intermediates in Aqueous Aerosol Microdroplets Exposed to a Reactive Gas. *J. Phys. Chem. A* **2007**, *111*, 13032−13037.
(93) Ingram, A. J.; Boeser, C. L.; Zare, R. N. Going Beyond Electrospray: Mass Spectrometric Studies of Chemical Reactions in and on Liquids. *Chem. Sci.* **2016**, *7*, 39−55.

DOI: 10.1021/acs.jpclett.7b00434
J. Phys. Chem. Lett. 2017, 8, 1615−1623